Catalysis Today 170 (2011) 20–26

Contents lists available at ScienceDirect

Catalysis Today

journal homepage: www.elsevier.com/locate/cattod

Enhanced hydrogen production by hydrolysis of $NaBH_4$ using "*Co-B nanoparticles supported on Carbon film*" catalyst synthesized by pulsed laser deposition

N. Patel*, R. Fernandes, N. Bazzanella, A. Miotello

Dipartimento di Fisica, Università degli Studi di Trento, Via sommarive 14, I-38123 Povo, Trento, Italy

ARTICLE INFO

Article history:
Received 25 October 2010
Received in revised form
25 November 2010
Accepted 27 November 2010
Available online 5 January 2011

Keywords:
H_2 generation
Sodium borohydride
Cobalt boride
Porous carbon film
Nanoparticles
Laser ablation

ABSTRACT

Co-B nanoparticles supported over carbon films were synthesized by using pulsed laser deposition (PLD) and used as catalysts in the hydrolysis of sodium borohydride ($NaBH_4$) to produce molecular hydrogen. Amorphous Co-B-based catalyst powders, produced by chemical reduction of cobalt salts, were used as target material for nanoparticles-assembled Co-B film catalysts preparation through PLD. Various Ar pressures (10–50 Pa) were used during deposition of carbon films to obtain extremely irregular and porous-carbon support with high surface area prior to Co-B film deposition. Surface morphology of the catalyst films was studied using scanning and transmission electron microscopy, while structural characterizations were carried out using X-ray diffraction. The hydrogen generation rate attained by carbon-supported Co-B catalyst film is significantly higher as compared to unsupported Co-B film and to conventional Co-B powder. Morphological analysis along with $NaBH_4$ hydrolysis tests showed that the Co-B nanoparticles produced with PLD act as active catalytic centers for hydrolysis while the carbon support provides high initial surface area for the Co-B nanoparticles with better dispersion and tolerance against aggregation. The hydrogen generation rate obtained by the present catalyst film was also investigated as a function of Co-B loading, carbon morphology, and solution temperature. The high performance of our carbon-supported Co-B film is well supported by the obtained very low activation energy (~31 kJ $(mol)^{-1}$) and exceptionally high H_2 generation rate (8.1 L H_2 min^{-1} (g of catalyst)$^{-1}$) in the hydrolysis of $NaBH_4$.

1. Introduction

Chemical hydrides ($NaBH_4$, NH_3BH_3, $LiBH_4$, NaH, KBH_4, etc.) with high hydrogen storage capacity in terms of gravimetric and volumetric efficiencies are the most prospective contenders to supply pure hydrogen at room temperature [1,2]. Among them, sodium borohydride ($NaBH_4$) has attracted worldwide interest mainly because it is stable in alkaline solution, non-flammable, non-toxic in nature, and with hydrogen storage capability of 10.8 wt%. [3]. Furthermore, hydrogen is generated by water-based hydrolysis reaction of $NaBH_4$ with the important advantage of producing half of the hydrogen from the water solvent. However, catalyst is required to accelerate this hydrolysis reaction in a controllable manner. Therefore, the catalyst is the key factor that affects the H_2 generation performance from hydrolysis of $NaBH_4$. Another limitation for the development of $NaBH_4$-based hydrogen technology is related to its regeneration from end product (borax), a process that still needs large amount of energy.

Solid state catalysts such as precious metals (generally functionalized with support) or transition metals and their salts are found to be very efficient in accelerating the hydrolysis reaction in a controllable manner. Noble catalysts like Pt [4] and Pd [5] supported on carbon, PtRu supported on metal oxide [6], Ru supported on anion-exchange resin [1], Rh supported on different materials [7], Ru nanoclusters [8], and Ru-promoted sulphated zirconia [9] have been utilized in the past to enhance the hydrogen production rate. However, these catalysts do not seem to be viable for industrial application considering their cost and availability. Transition metals such as fluorinated Mg based alloy [10], Raney Ni and Co, nickel and cobalt borides [11–13], and even metal salts are generally used to accelerate the hydrolysis reaction of $NaBH_4$. Metal-boride amorphous alloy catalysts, prepared by reduction of metal salts with a reducing agent, have attracted much attention in catalysis field owing to their unique properties such as isotropic structure and high concentration of coordinative unsaturated sites [14,15]. For these reasons, Cobalt boride (Co-B) is considered, among all the above mentioned catalysts, as an excellent candidate for the H_2 production by catalytic hydrolysis of $NaBH_4$, also owing to its relevant chemical stability and low cost. Generally in the past, Co-B catalyst was studied in form of homogeneous powder which has however the problem related to separation and aggregation. On

* Corresponding author.
E-mail address: patel@science.unitn.it (N. Patel).

0920-5861/$ – see front matter © 2010 Elsevier B.V. All rights reserved.
doi:10.1016/j.cattod.2010.11.077

the other hand, Co-B in form of thin films will serve as an environmentally friendly *"green catalyst"* for being easily recovered, reused, and acting as suitable tool for on/off switch. This thin film catalyst can also acquire better catalytic properties because of the inherent surface morphology and structure. In our previous works [13,16,17], Co-B catalysts synthesized by pulsed laser deposition (PLD) in form of nanoparticle-assembled films showed a high performance for hydrogen production in catalytic hydrolysis reaction of NH_3BH_3 and $NaBH_4$. However this nanoparticle-assembled film was deposited on flat glass surface which does not exhibit the required features of a large-surface area support intended for catalysis process.

Supports such as carbon, silica, and alumina play not merely the role of carrier for active metal, but also provide a large active surface area and better dispersion of the active phase due to their porous nature. Besides that, a supported catalyst facilitates the diffusion of reactants through the pores to the active phase, improves the dissipation of the reaction heat, retards the sintering of the active phase, and increases the poison resistance. Carbon appears the best support for active catalyst just because of its highly chemical inert nature particularly in strong basic and acid environments as well as good interaction with the active metals; finally it also provides flexibility to produce selected morphology and porosity [18]. The presence of oxygen-containing groups on the carbon surface which can be acidic, neutral, and basic in nature, has also a great effect on the absorptive properties [19]. In our previous work, we deposited cluster-assembled C-films having structure ranging from diamond-like to highly porous form, by PLD using a range of laser parameters [20]. Thin Pd layer deposited on top of these C-films were later utilized as catalyst for H_2 generation by hydrolysis of $NaBH_4$ and showed significantly superior activity as compared to unsupported Pd: we attributed this feature to the high dispersion of active Pd particles provided by the morphology of C-films [21,22].

The aim of the present work is to study the effect of morphological properties of carbon films, produced by PLD under different Ar gas pressures, as a support for the nanoparticles-assembled Co-B film catalyst. The C-supported Co-B film shows much improved performance for catalytic hydrolysis of $NaBH_4$ solution to produce hydrogen. The results are discussed in terms of active nature of Co-B nanoparticles and high surface area provided by the carbon films.

2. Experimental

Co-B powder catalyst, synthesized by the chemical reduction method, was used as the target material for the deposition of catalyst film by PLD. This powder was prepared by adding sodium borohydride, used as reducing agent, to an aqueous solution (0.05 M) containing cobalt salt ($CoCl_2$) under vigorous stirring. The black powder separated from the solution during reaction course was filtered and then extensively washed with distilled water and ethanol before drying at around 323 K under continuous N_2 flow. In order to be used as a target for the film deposition, the Co-B powder was cold pressed in form of cylindrical disks. PLD was performed using KrF excimer laser (Lambda Physik) at the operating wavelength of 248 nm, pulse duration of 25 ns, and repetition rate of 30 Hz. According to our previous experience [13,16], the ablation of Co-B was carried out under vacuum condition with a base pressure of 2×10^{-5} Pa by using laser pulses of 3 J/cm^2. The target to substrate distance was maintained at 4 cm. Details of the deposition apparatus are reported in Ref. [23].

Co-B film supported on carbon was synthesized in two steps: (1) by first depositing carbon film by PLD, on a glass substrate, using a laser fluence of 12 J/cm^2 and varying Ar pressure from 10 to 50 Pa to obtain different surface roughness; (2) by PLD of Co-B nanoparticles-assembled film over these carbon substrates in vacuum with same laser parameters as used to deposit unsupported Co-B film. Weight of the catalyst loading was evaluated by measuring the weight of the glass slide (76 mm × 46 mm) with carbon film, before and after deposition of Co-B film: it was kept approximately constant for all the produced samples (10 mg). Films were deposited on silicon substrates for the characterization and on glass substrates to test their catalytic activity.

The surface morphology of all catalyst powders was studied by scanning electron microscope (SEM-FEG, JSM 7001F, JEOL) equipped with energy-dispersive spectroscopy analysis (EDS, INCA PentaFET-x3) to determine the composition of the samples. Transmission electron microscopy (TEM) analyses were performed with a field emission FEI TECNAI F20 SuperTwin FEG-(S)TEM microscope operating at 200 kV equipped with an EDAX energy-dispersive X-ray spectrometer (EDS). Structural characterization of the catalyst powders was carried out by conventional X-ray diffraction (XRD) using the Cu K_α radiation (λ = 1.5414 Å) in Bragg–Brentano (θ–2θ) configuration.

For catalytic activity measurements, an alkaline-stabilized solution of sodium borohydride (pH 13, 0.025 ± 0.001 M) (Rohm and Haas) was prepared by addition of NaOH. The titre of reagent was independently measured through iodometric method [24]. The generated hydrogen quantity was measured through a gas volumetric method in an appropriate reaction chamber with thermostatic bath, wherein the temperature was kept constant within accuracy±0.1 K. The chamber was equipped with pressure sensor, stirrer system, catalyst insertion device, and also coupled with an electronic precision balance to accurately measure the weight of water displaced by the hydrogen produced during the reaction course. A detailed description of the measurement apparatus is reported in Ref. [25]. In all the runs, the catalyst was placed on the appropriate device inside the reaction chamber and the system was sealed. Catalyst powder or film was added to 200 ml of the above solution, at 298 K, under continuous stirring. In order to make comparison, the H_2 cumulative production yield (%) versus time was plotted instead of the hydrogen volume (ml) versus time. The efficiency of the all form of catalysts was compared by using analogous amount of Co-B catalyst (∼10 mg). The H_2 generation rate was measured at different temperatures to determine the activation energy involved in the catalytic hydrolysis reaction.

3. Results and discussion

In our previous works [13,16,21,22], we have successfully developed by PLD two kinds of catalyst films for catalytic hydrolysis of $NaBH_4$ solution to generate pure H_2 gas. These catalysts were in form of Co-B nanoparticles-assembled thin film and Pd supported on rough carbon thin film. Both these catalyst films showed excellent activity to produce expected amount of H_2 from hydrolysis of $NaBH_4$ with significantly higher rates (about 5–6 times) than the same amount of the corresponding powders. For Co-B film, the enhanced catalytic activity was mainly attributed to the Co-B nanoparticles, produced during the ablation process on the film surface, with average size of around ∼250 nm and well established spherical form [13,16]. These nanoparticles not only increase the surface area of the catalyst but also act as the active catalytic centers for the hydrolysis reaction of $NaBH_4$. In the case of Pd/C film, the highly porous and irregular morphology of carbon support provides very high initial surface area and better dispersion of Pd particles on the surface [21,22]. These results showed that Co-B nanoparticles and appropriate carbon film morphology were the main reason behind the enhanced performance of Co-B and Pd/C thin film catalysts. Considering our previous results, in the present work we combine the two features (nanoparticles and rough sup-

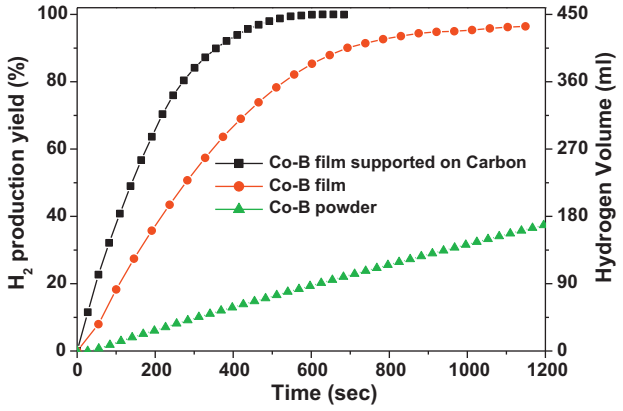

Fig. 1. Hydrogen generation yield as a function of reaction time obtained by hydrolysis of alkaline $NaBH_4$ solution (0.025 M) with Co-B catalyst powder and with unsupported and C-supported Co-B film deposited by PLD. Carbon film used for the measurement was deposited with Ar pressure of 40 Pa.

port surface) to synthesize Co-B nanoparticles on highly irregular and porous carbon film support to improve the initial surface area and obtain better dispersion of nanoparticles. Carbon film was deposited on the glass substrate using Ar gas pressure (40 Pa) in the PLD chamber prior to the deposition of Co-B film.

Hereafter Co-B film deposited on glass substrate and on carbon film will be designated as unsupported- and C-supported Co-B film, respectively. The catalytic activity of C-supported and unsupported Co-B film was compared by measuring the hydrogen generation yield as function of time by hydrolysis of alkaline $NaBH_4$ (0.025 M) solution at 298 K: results are reported in Fig. 1. The figure clearly shows that both the Co-B catalyst films are really efficient and produce hydrogen instantaneously as soon as they come in contact with the $NaBH_4$ solution. However, the C-supported Co-B film exhibits higher catalytic activity as compared to the unsupported Co-B film and it was able to complete the reaction within 10 min while the same amount of unsupported Co-B film catalyst (~10 mg) takes about 18 min and the Co-B powder catalyst takes 85 min. The expected total amount of H_2 was measured irrespective of the type of used catalyst. The H_2 generation yield values reported in Fig. 1 are perfectly fitted by using a single exponential function [26], as described by:

$$[H_2](t) = [H_2]_{max} \times (1 - e^{-k_1 t}) = 4[[BH_4^-]_0 \times (1 - e^{-k_1 t})] \quad (1)$$

where $[BH_4^-]_0$ is the initial molar concentration of $NaBH_4$ in the solution and k_1 is the overall rate constant of the reaction. This indicates that hydrolysis reaction is first order reaction with respect to $NaBH_4$. In the present case a low hydride/catalyst ratio was used which means that the first order kinetics involving diffusion of BH_4^- on the catalyst surface is the rate limiting step during the hydrolysis reaction (see discussion reported in Ref. [26]).

A numerical procedure, described elsewhere [16], was utilized to obtain the maximum value of the hydrogen generation rate (R_{max}) for all the catalysts. By using same catalyst amount (10 mg), the maximum H_2 generation rate obtained for C-supported Co-B films (~8100 ml/min/g catalyst) has been found significantly higher (almost 2 times) than that obtained using the unsupported Co-B film (~4330 ml/min/g catalyst). While the R_{max} value for C-supported Co-B films is about one order of magnitude higher than Co-B powder catalyst (~850 ml/min/g catalyst). Several films synthesized by using the same PLD parameters showed almost identical (±5%) H_2 generation rate, thus establishing the reproducibility of our produced PLD films. During the reaction, the catalyst films were quite stable both in terms of hydrogen-production and bonding with the substrate.

Structural characterization by XRD (not reported) shows that both unsupported- and C-supported-Co-B catalyst films synthesized by PLD are amorphous in nature. In Fig. 2 we present SEM images of Co-B catalyst powder and of both films (unsupported and C-supported) synthesized by PLD. The SEM images of catalyst powders show typical particle-like morphology with spherical shape and average size of a few nanometers. However, because of the high surface energy related to these particles, they tend to agglomerate as observed in the SEM image (Fig. 2a). As seen in Fig. 2b, the surface of unsupported Co-B catalyst films exhibit a nanoparticles-assembled structure made of well dispersed spherical particles with size ranging between 50 and 300 nm. In addition to this Co-B nanoparticles, we also observed much smaller Co nanoparticles (NPs) embedded in boron matrix on the film surface by TEM. Fig. 3a represents the bright-field TEM micrographs of Co-B film surface deposited by PLD using laser fluencies of 3 J/cm^2. The Co-NPs, with well defined spherical shape and average size of 11 ± 4 nm, are observed to be well-dispersed in the matrix of light element (especially boron or boron-oxide) as confirmed by energy dispersive X-ray spectroscopy. The histograms of particle size distribution are illustrated in Fig. 3b, while the particle density (with size $D < 30$ nm) calculated from this plot is about 320 ± 30 NP/μm^2.

Depending on the laser energy density and target material thermodynamic properties, the laser ablation process falls into two main categories: vaporization (also intense vaporization) and explosive boiling [27,28]. The mechanism of direct nanoparticle formation is here attributed to the phase explosion process that occurs under extreme conditions of high temperature and pressure produced by the laser pulses irradiating targets in vacuum [29]. High energy density laser beam irradiation causes a superheating of the region below the target surface beyond the limit of thermodynamic stability of the material (~90% of the thermodynamic critical temperature, T_c) inducing a homogeneous nucleation of vapor bubble. The target surface then makes a rapid transition from superheated liquid to a matrix of vapor and liquid nano-size droplets, which leave the irradiated target surface and get deposited on the substrate: this is the case for Co-B nanoparticles (50–300 nm range) formation on the surface. The phase explosion process occurs in a superheated liquid near T_c and we suppose that the emitted liquid would have a homogeneous Co-B composition. However, either during the flight from target to substrate, or just on the substrate, cooling processes will occur that could lead to phase separation and Co NP formation within the boron matrix occurs on the surface. However, the involved mechanisms are still under investigation.

SEM images of C-supported Co-B film (Fig. 2c) show dendritic microstructure of carbon film with highly irregular and porous surface. To clearly identify Co-B particles in carbon film the compositional SEM image in backscattering electron mode (BSE) was acquired (Fig. 2d). In BSE images materials of heavy and light elements can be readily distinguished through their brightness. Thus from Fig. 2d, it is clearly evident the presence of Co-B nanoparticles (bright particles) embedded in the porous carbon film with improved dispersion. The mechanism behind the formation of such rough carbon surface through PLD is discussed below.

The above morphological results confirm our previous finding that the enhanced catalytic activity obtained with Co-B film, as compared to powder, is primarily attributed to the Co-B nanoparticles which act as active catalytic centers for the hydrolysis reaction. Depositing these active Co-B nanoparticles on carbon film gives rise to a further enhancement in catalytic activity which is mostly ascribed to highly rough and porous carbon surface which: (1) favors the better dispersion of the nanoparticles, (2) provides high initial surface area, and (3) stabilizes the nanoparticles against aggregation. To further confirm the role of carbon film we used different Ar pressure in PLD chamber, ranging from 10 to 50 Pa, to tailor roughness of deposited C-films.

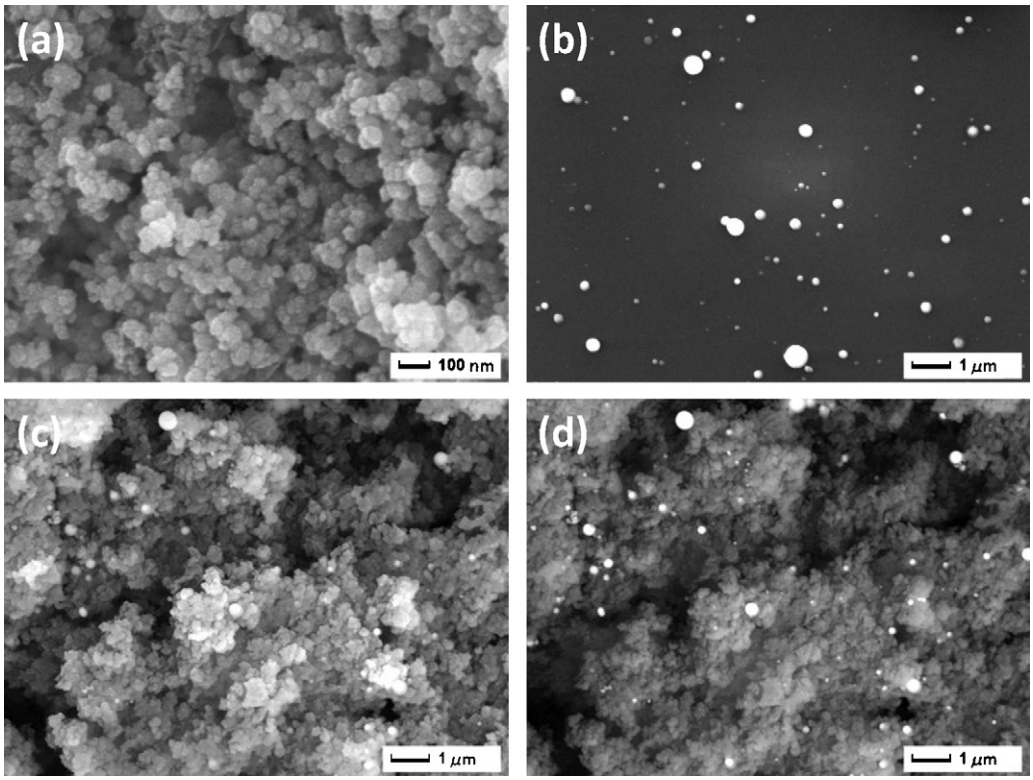

Fig. 2. SEM micrographs of Co-B catalyst: (a) powder, (b) unsupported film, and (c) C-supported film deposited by PLD. (d) Back scattering electron image of C-supported Co-B film. Carbon film used for the measurement was deposited with Ar pressure of 40 Pa.

The SEM images of the carbon films deposited under Ar gas pressure of 20, 30, 40 and 50 Pa are illustrated in Fig. 4a, c, e and g, while Co-B film supported on these carbon films are reported in Fig. 4b, d, f and h, respectively. Microstructures ranging from flat to highly irregular and to porous are clearly visible. The carbon film deposited at low Ar pressure (20 Pa) exhibits columnar structure (observed through cross-section SEM images of the film, figure not shown) with embedded spherical nodules on the surface. By increasing the pressure (to 30 and 40 Pa) dendritic, highly porous microstructure starts to appear with extremely irregular surface. The nodes in this case appear bigger, loosely packed, and non-spherical. Film-substrate adhesion is slightly poor than that reached at low Ar pressure. When using high pressure conditions (50 Pa), the film appears powder-like, with barely any adhesion to the substrate. The morphology of such a film is very similar to that of simulated films grown under ballistic deposition conditions. The collisional effects imposed by inert gas (Ar) at high pressure in the deposition chamber cause a cooling down of plume along with charges recombination and condensation of carbon clusters in the plume which are deposited on the substrate. In particular, by increasing the gas pressure, cluster–cluster collision may also occur that contributes to formation of bigger clusters which, when assembled, form highly porous and irregular structure on the film surface. The visible consequence of such a process is the peculiar sequence of morphologies that develop in the growing film as discussed in Ref. [18].

Hydrogen generation yield was measured, as a function of time, during the hydrolysis of alkaline $NaBH_4$ solution (0.025 M) at 298 K in presence of Co-B film catalyst supported on different carbon films deposited with various Ar pressures ranging from 10 to 50 Pa

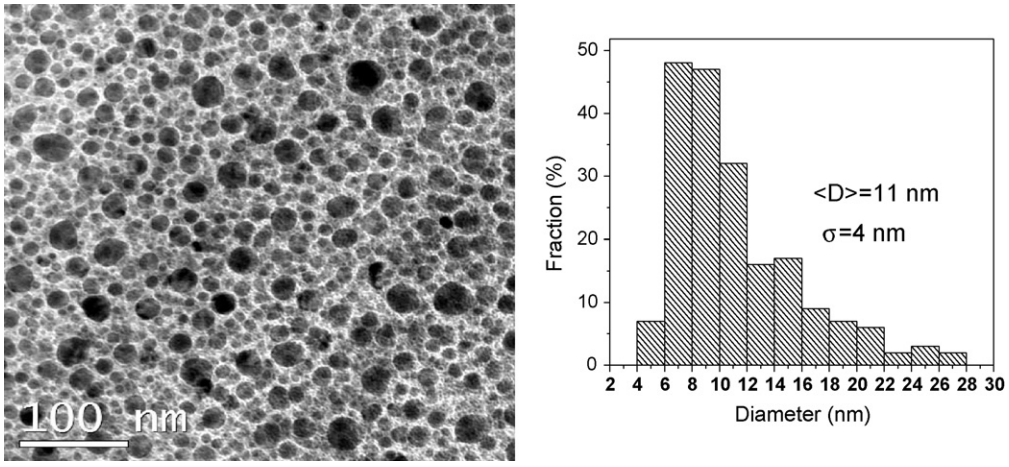

Fig. 3. (a) Bright field TEM images and (b) particle size histogram for unsupported Co-B catalyst film deposited by PLD using energy density of 3 J/cm^2.

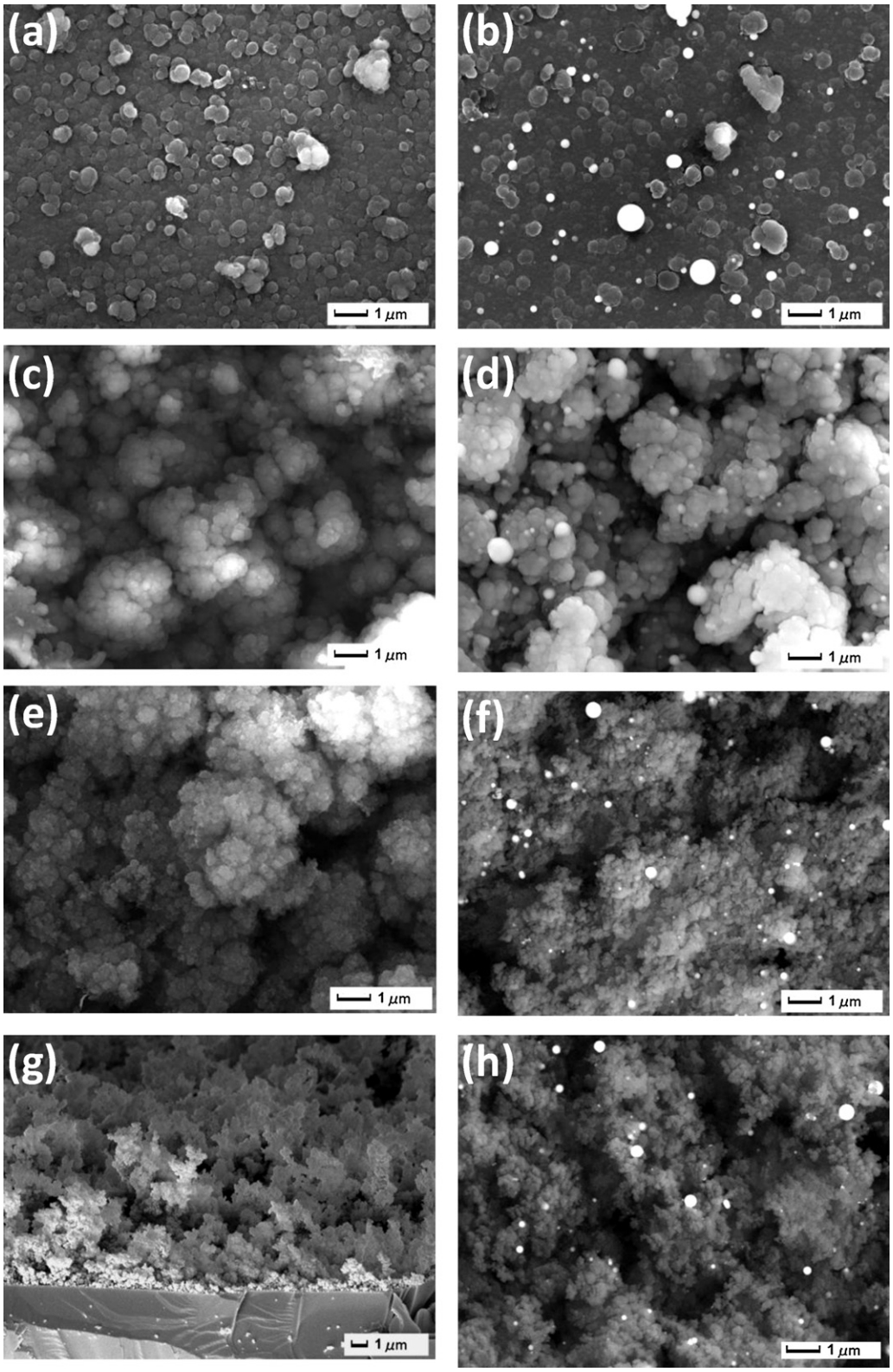

Fig. 4. SEM micrographs of the carbon films deposited under different Ar gas pressures (a) 20, (c) 30, (e) 40 and (g) 50 Pa, while (b), (d), (f) and (h) are the SEM images of Co-B film supported on these carbon films, respectively.

(Fig. 5). The inset of Fig. 5 shows the R_{max} as a function of Ar gas pressure used to deposit the carbon films. Co-B catalysts supported on C-film deposited at low Ar pressures (10 and 20 Pa) show almost similar catalytic activity as un-supported Co-B film. We attribute this result to the non-porous structure of C-films. However, the catalytic activity increases for Co-B catalysts supported on C-films deposited at higher Ar pressures (30 and 40 Pa). R_{max} reached the maximum for C-film deposited at 40 Pa. As indicated by SEM images, the roughness and surface area of C-film increases with the deposition pressure. This trend is also followed by the

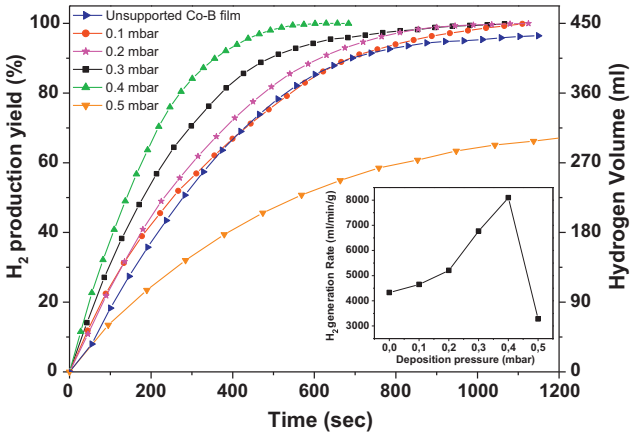

Fig. 5. Hydrogen generation yield as a function of reaction time obtained by hydrolysis of alkaline $NaBH_4$ solution (0.025 M) with Co-B film catalyst supported on carbon films deposited with various Ar pressures by PLD. Inset shows the R_{max} as a function of Ar gas pressure used to deposit the carbon films.

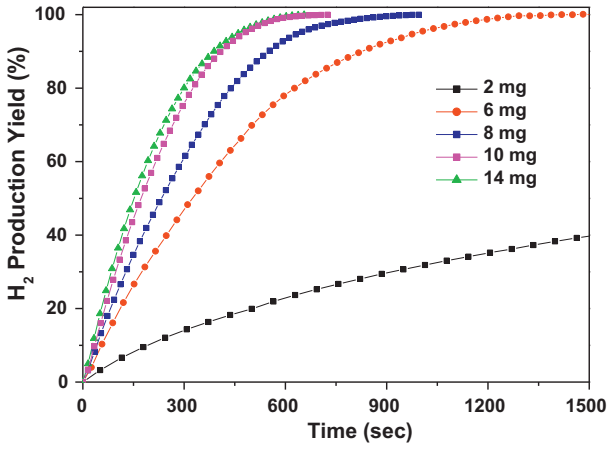

Fig. 7. Hydrogen generation yield as a function of reaction time obtained by hydrolysis of alkaline $NaBH_4$ solution (0.025 M) at 298 K in presence of Co-B catalyst with different loadings (2, 6, 8, 10, 14 mg) on carbon film support (40 Pa).

H_2 generation rate for hydrolysis of $NaBH_4$ as demonstrated in the inset of Fig. 5. Thus, surface area and roughness of C-films play a vital role in the increment of catalytic activity for Co-B film catalyst by providing better dispersion and avoiding aggregation of Co-B nanoparticles. On the contrary, Co-B catalyst supported on C-film deposited at highest pressure of 50 Pa shows a drastic decrease in the H_2 generation rate and was not able to complete the hydrolysis reaction of $NaBH_4$. The C-film deposited at this pressure has a very week adhesion with the substrate and thus, under vigorous stirring, the carbon film slowly detached from the substrate and agglomerates into big clusters in the reactant solution during the $NaBH_4$ hydrolysis reaction. These carbon clusters completely enclose the Co-B nanoparticles inside, thus causing the major retardation in H_2 generation rate.

In Fig. 6 the H_2 generation yields, obtained through hydrolysis of alkaline $NaBH_4$ (0.025 M) solution using C-supported Co-B film, are reported as a function of time at different reaction temperatures. The carbon film deposited with Ar pressure of 40 Pa was used for the measurement. The Arrhenius plot of the hydrogen production rates (inset of Fig. 6) gives an activation energy value of 31 ± 2 kJ mol^{-1} for C-supported nanoparticles-Co-B film which is the same as that obtained with unsupported nanoparticles-Co-B film (30 ± 1 kJ mol^{-1}) but much lower than that of Co-B powder (45 ± 1 kJ mol^{-1}) [30]. In general, the obtained

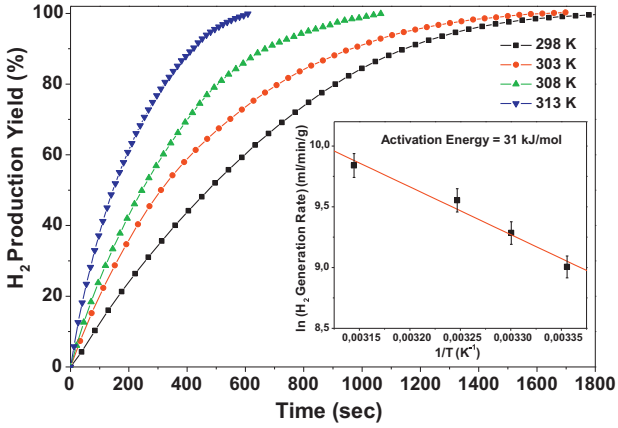

Fig. 6. Hydrogen generation yield as a function of reaction time obtained by hydrolysis of alkaline $NaBH_4$ solution (0.025 M) with C-supported (40 Pa) Co-B film catalyst measured at 4 different solution temperatures. Inset shows the Arrhenius plot of the H_2 generation rates.

activation energies are lower than that obtained with Co-B supported on different materials such as carbon (57.8 kJ mol^{-1}) [31], carbon nano-tubes (MWCNT) (40.4 kJ mol^{-1}) [32], and Ni foam (33 kJ mol^{-1}) [33]. The present value is also lower than that of Co-based catalyst for example Raney Co (53.7 kJ mol^{-1}) [34], Co-B nanoparticles (42.7 kJ mol^{-1}) [35], Co supported on activated carbon (44 kJ mol^{-1}) [36], structured Co_2B (45 kJ mol^{-1}) [37], Co-B thin film (44.47 kJ mol^{-1}) [38] and Co supported on γ-Al_2O_3 (33 kJ mol^{-1}) [39], The values are also lower than that found by Amendola (47 kJ mol^{-1}) [1] using Ru catalyst and by Kaufman and Sen [40] using different bulk metal catalysts, obtained 75 kJ mol^{-1} for cobalt, 71 kJ mol^{-1} for nickel, and 63 kJ mol^{-1} for Raney nickel. The activation energy values obtained in the present case are comparable to that obtained with Pd/C powder (28 kJ mol^{-1}) [21], Ru nanoclusters (29 kJ mol^{-1}) [8] and Ru–C (37 kJ mol^{-1}) [41]. The favorable activation energy values obtained in the present work are attributed to active nature of Co-B nanoparticles which are well dispersed in porous carbon film that indeed provides the initial high surface area and avoids agglomeration thus enhancing the catalytic hydrolysis reaction.

The effect of catalyst loading on catalytic activity of Co-B/C catalyst was studied by depositing different amount of Co-B catalyst on carbon film (deposited with 40 Pa Ar pressure). Fig. 7 presents the hydrogen generation yield, as a function of time, occurring from the hydrolysis of alkaline $NaBH_4$ solution (0.025 M) at 298 K in presence of Co-B catalyst with different amount of loading (2, 6, 8, 10, 14 mg) on carbon film support. It is observed that H_2 generation rate (H_2 ml/min) increases with Co-B loading and takes less amount of time to produce the expected amount of H_2. However for higher Co-B loading, more than 10 mg, no further increment in H_2 generation rate is observed. This result shows that 10 mg is enough to cover the carbon film with better dispersion of NPs while high loading might decrease the level of dispersion.

4. Conclusion

Co-B NPs supported on carbon films were synthesized by using PLD and used as catalysts in the hydrolysis of $NaBH_4$ to produce H_2. Several Ar pressures, in the range from 10 to 50 Pa, were used during PLD of carbon films to tailor roughness and porosity of carbon support prior to PLD of Co-B film. The hydrogen generation rate attained with carbon-supported Co-B catalyst film (Ar pressure of 40 Pa for C deposition) is significantly higher (8.1 L H_2 min^{-1} (g of catalyst)$^{-1}$) as compared to unsupported Co-B film (~4.33 L H_2 min^{-1} (g of catalyst)$^{-1}$) and to conventional Co-

B powder ($\sim$0.85 L H_2 min^{-1} (g of catalyst)$^{-1}$). SEM analysis along with $NaBH_4$ hydrolysis tests show that the Co-B NPs act as active catalytic centers for hydrolysis while the carbon support provides both better dispersion of the Co-B NPs and atomic barriers that avoid NPs aggregation. The hydrogen generation rate obtained by the present carbon-supported Co-B catalyst was also investigated as a function of Co-B loading and solution temperature. The H_2 generation rate increases as function of loading but no further increment is observed for loading exceeding 10 mg that is indeed enough to cover the carbon film with the best dispersion of NPs. Finally, the high performance of our carbon-supported Co-B film is well supported by the obtained very low activation energy ($\sim$31 kJ (mol)$^{-1}$) in the hydrolysis of $NaBH_4$.

Acknowledgements

We thank C. Armellini for XRD analysis, G. Mattei for TEM analysis, and G. Guella for discussion of the results. The research activity is financially supported by "Fondazione Cassa di Risparmio di Trento e Rovereto".

References

[1] S.C. Amendola, S.L. Sharp-Goldman, M.S. Janjua, N.C. Spencer, M.T. Kelly, P.J. Petillo, M. Binder, Int. J. Hydrogen Energy 25 (2000) 969.
[2] R.B. Biniwale, S. Rayalu, S. Devotta, M. Ichikawa, Int. J. Hydrogen Energy 33 (2008) 360.
[3] S.C. Amendola, S.L. Sharp-Goldman, M.S. Janjua, M.T. Kelly, P.J. Petillo, M. Binder, J. Power Sources 85 (2000) 186.
[4] Y. Bai, C. Wu, F. Wu, B. Yi, Mater. Lett. 60 (2006) 2236.
[5] G. Guella, C. Zanchetta, B. Patton, A. Miotello, J. Phys. Chem. B 110 (2006) 17024.
[6] P. Krishnan, T.H. Yang, W.Y. Lee, C.S. Kim, J. Power Sources 143 (2005) 17.
[7] V.I. Simagina, P.A. Storozhenko, O.V. Netskina, O.V. Komova, G.V. Odegova, Y.V. Larichev, A.V. Ishchenko, A.M. Ozerova, Catal. Today 138 (2008) 253.
[8] S. Özkar, M. Zahmakiran, J. Alloys Compd. 404–406 (2005) 728.
[9] U.B. Demirci, F. Garin, Catal. Commun. 9 (2008) 1167.
[10] S. Suda, Y.M. Sun, B.H. Liu, Y. Zhou, S. Morimitsu, K. Arai, N. Tsukamoto, M. Uchida, Y. Candra, Z.P. Li, Appl. Phys. A: Mater. Sci. Process. 72 (2001) 209.
[11] B.H. Liu, Z.P. Li, S. Suda, J. Alloys Compd. 415 (2006) 288.
[12] S.U. Jeong, E.A. Cho, S.W. Nam, I.H. Oh, U.H. Jung, S.H. Kim, Int. J. Hydrogen Energy 32 (2007) 1749.
[13] N. Patel, G. Guella, A. Kale, A. Miotello, B. Patton, C. Zanchetta, L. Mirenghi, P. Rotolo, Appl. Catal. A: Gen. 323 (2007) 18.
[14] A. Baiker, Faraday Discuss. Chem. Soc. 87 (1989) 239.
[15] Y. Pei, P. Guo, M. Qiao, H. Li, S. Wei, H. He, K. Fan, J. Catal. 248 (2007) 303.
[16] N. Patel, R. Fernandes, G. Guella, A. Kale, A. Miotello, B. Patton, C. Zanchetta, J. Phys. Chem. C 112 (2008) 6968.
[17] N. Patel, R. Fernandes, G. Guella, A. Miotello, Appl. Catal. B: Environ. 95 (2010) 137–143.
[18] F. Rodriguez-Reinoso, Carbon 36 (1998) 159.
[19] F. Rodriguez-Reinoso, M. Molina-Sabio, A.M. Munecas, J. Phys. Chem. 96 (1992) 2707.
[20] P.M. Ossi, C.E. Bottani, A. Miotello, Thin Solid Films 482 (2005) 2.
[21] N. Patel, B. Patton, C. Zanchetta, R. Fernandes, G. Guella, A. Kale, A. Miotello, Int. J. Hydrogen Energy 33 (2008) 287.
[22] N. Patel, R. Fernandes, G. Guella, A. Kale, A. Miotello, B. Patton, C. Zanchetta, P.M. Ossi, V. Russo, Appl. Surf. Sci. 254 (2007) 1307.
[23] M. Bonelli, C. Cestari, A. Miotello, Meas. Sci. Technol. 10 (1999) N27.
[24] D.A. Lyttle, E.H. Jensen, W.A. Struck, Anal. Chem. 24 (1952) 1843.
[25] C. Zanchetta, B. Patton, G. Guella, A. Miotello, Meas. Sci. Technol. 18 (2007) N21.
[26] N. Patel, R. Fernandes, A. Miotello, J. Power Sources 188 (2009) 411.
[27] A. Miotello, R. Kelly, Appl. Phys. Lett. 67 (1995) 3535.
[28] L.V. Zhigilei, Z. Lin, D.S. Ivanov, J. Phys. Chem. C 113 (2009) 11892.
[29] R. Kelly, A. Miotello, Appl. Surf. Sci. 96–98 (1996) 205.
[30] R. Fernandes, N. Patel, A. Miotello, M. Filippi, J. Mol. Catal. A: Chem. 298 (2009) 1.
[31] J. Zhao, H. Ma, J. Chen, Int. J. Hydrogen Energy 32 (2007) 4711.
[32] Y. Huang, Y. Wang, R. Zhao, P.K. Shen, Z. Wei, Int. J. Hydrogen Energy 33 (2008) 711.
[33] H.B. Dai, Y. Liang, P. Wang, H.M. Cheng, J. Power Sources 177 (2008) 17.
[34] B.H. Liu, Z.P. Li, S. Suda, J. Alloys Compd. 415 (2006) 288.
[35] A. Garron, D. Swierczynski, S. Bennici, A. Auroux, Int. J. Hydrogen Energy 34 (2009) 1185.
[36] D. Xu, P. Dai, X. Liu, C. Cao, Q. Guo, J. Power Sources 182 (2008) 616.
[37] J. Lee, K.Y. Kong, C.R. Jung, E. Cho, S.P. Yoon, J. Han, T.G. Lee, S.W. Nam, Catal. Today 120 (2007) 305.
[38] P. Krishnan, S.G. Advani, A.K. Prasad, Appl. Catal. B: Environ. 86 (2009) 137.
[39] W. Ye, H. Zhang, D. Xu, L. Ma, B. Yi, J. Power Sources 164 (2007) 544.
[40] C.M. Kaufman, B. Sen, J. Chem. Soc., Dalton Trans. 2 (1985) 307.
[41] Y. Shang, R. Chen, Energy Fuels 20 (2006) 2149.